A Unified Model Predictive Voltage and Current Control for Microgrids with Distributed Fuzzy Cooperative Secondary Control

Yinghao Shan, Jiefeng Hu, *Senior Member, IEEE*, Ka Wing Chan, and Syed Islam, *Fellow, IEEE*

Abstract—A microgrid formed by a cluster of parallel distributed generation (DG) units is capable of operating in either islanded mode or grid-connected mode. Traditionally, by using model predictive control (MPC) algorithms, these two operation modes can be achieved with two separate and different cost functions, which brings in control complexity and hence, compromises system reliability. In this paper, a unified model predictive voltage and current control (UMPVIC) strategy is proposed for both islanded and grid-connected operations and their smooth transition. The cost function is kept unified with voltage and current taken into account without altering the control architecture. It can be used for high-quality voltage supply at the primary control level and for bidirectional power flow at the tertiary control level. In addition, by only using DGs' own and neighboring information, a distributed fuzzy cooperative algorithm is developed at the secondary layer to mitigate the voltage and frequency deviations inherent from the power droop. The fuzzy controller can optimize the secondary control coefficients for further voltage quality improvement. Comprehensive tests under various scenarios demonstrate the merits of the proposed control strategy over traditional methods.

Index Terms--Model predictive control, distributed fuzzy secondary control, droop control

I. INTRODUCTION

Microgrids, as the key building blocks of the smart grid, form flexible interfaces between the main power network and the distributed generation (DG) units such as solar photovoltaic (PVs), wind turbines and energy storage systems. In the last few years, the hierarchical control has been a widely recognized standard framework for various microgrids [1, 2]. In islanded mode, since it is independent of the main grid, the microgrid operates as an integral entity in which the frequency and voltage should be regulated internally and locally. This is crucial for a majority of microgrids, especially for those built in rural areas where power users require a high level of reliability.

Once the microgrid is grid-connected, the system frequency and voltage are strongly supported by the stiff grid. In this case, microgrids supply extra power and participate in energy scheduling of the power system. In case of grid faults or outages, the microgrid can be cut off with an islanding action to form a self-sufficient entity as quickly as possible. Thus, it is extremely crucial to formulate appropriate control methods for microgrids to achieve stable and efficient multi-mode operations between islanded and grid-connected modes as well as their transitions.

So far, much effort has been devoted to realizing the multi-mode operations of AC microgrids. In [3-5], the improvement is only made on droop control method, while the voltage and current dual loops based on cascaded linear control technique are remained unchanged to produce pulse-width modulation (PWM) signals. For [6], voltage control loop and current control loop are respectively adopted for different operation modes. In [7], a PV-battery-based microgrid is studied. Similarly, the dual control loops are again kept for signal generation. In [8, 9], cascaded linear control loops are developed to transfer different modes. However, conventional cascaded control structure needs superposed nested loops and time-consuming proportional-integral-derivative (PID) parameter tuning to realize multi-functionalities, and it is difficult to include variable constraints. It therefore lacks sufficient control flexibility and intelligence in renewable energy and microgrids with multiple control layers and multiple objectives.

In clear contrast to cascaded linear loops, model predictive control (MPC) computes the optimal control command through minimizing a preset cost function and the target system model. This computation completes at each sampling time over a certain time interval. Recently, MPC has shown an increasing trend in microgrid control regarding multi-mode operations due to its specific features like a rapid response, free of complex tuning procedure, and removal of PWM generators as well as ease to involve various constraints. In [10-12], MPC is used only in islanded microgrids attempting to achieve a better performance. While in [13-15], when the microgrid operation mode alters, they have to significantly change the control target. So far, it has not been sought to develop a common format for these modes, thus to achieve a neat and integrated control to deal with the mode changes. In addition, in these studies, only the voltage magnitude error is considered in the cost function in islanded mode, which presents an inferior performance in terms of the voltage supply [10].

Another concern of microgrids is the power quality. In the microgrid's hierarchy, secondary control is used to eliminate the frequency/voltage deviations caused by the primary control. Among secondary controls, centralized control exposes potential

J. Hu and S. Islam are with the School of Engineering, IT and Physical Sciences, Federation University Australia, Mt Helen VIC 3353, Australia (email: j.hu@federation.edu.au; s.islam@federation.edu.au)
K. Chan is with the Department of Electrical Engineering, The Hong Kong Polytechnic University, Hong Kong SAR (email: eekwchan@polyu.edu.hk)

single point of failure and low scalability, while the distributed cooperative control based on sparse communication networks presents more reliability, robustness and flexibility [16]. Using distributed cooperative principle, the system only requires local or adjacent information without a central controller. In recent years, distributed cooperative secondary control have been increasingly applied to microgrids [17-23]. For example, in [17] and [18], the frequency and voltage of all DGs can reach consensus by using a distributed cooperative secondary control derived from the feedback linearization. In [21], a finite-time secondary frequency control approach is proposed to eliminate the frequency with fast convergence speed. However, the design of the secondary control coefficients in these studies lacks sufficient investigation. And, it is rare to see any existing work exploring the dynamic adjustment of the distributed secondary control coefficients to optimize the voltage/frequency deviation mitigation and dynamic response. It is therefore urgently needed to develop a self-adaptive mechanism to improve the secondary control.

To fill the aforementioned technical gaps, this paper proposes a unified model predictive voltage and current control (UMPVIC) architecture for microgrid multi-mode operations where the control structure is kept unchanged. In islanded operation, it enables proper load sharing among DGs with high-quality voltage supply. In grid-connected mode, it achieves flexible active and reactive power exchange with the main grid, which caters the recent grid code requirement for distributed energy systems. The proposed control method can also facilitate the smooth transition between operation modes. Then, a dynamically adjustable distributed cooperative method based on an effectively applicable fuzzy control logic is developed to restore the voltage and frequency. The overall control strategy is implemented in a hierarchical structure. Specifically, the proposed UMPVIC strategy integrated with droop scheme is used for primary control (and partly for the tertiary control). The fuzzy optimized distributed cooperative control is adopted at the secondary control layer. In summary, the main contributions of this paper are summarized as follows:

1) The proposed UMPVIC strategy can maintain a unified control structure in various operation modes in microgrids. By also taking into account the inductor current in addition to the capacitor voltage, a high-quality voltage is generated in islanded mode. Meanwhile, the bidirectional power flows are also achieved in grid-connected mode. In particular, the factors that impact voltage supply quality using MPC method in islanded mode is revealed and analyzed.

2) In existing distributed cooperative secondary control, the dynamic adjustment of the distributed secondary control coefficients has not been explored. We propose a mechanism to dynamically regulate the coefficients of distributed cooperative secondary control according to an explicit and intuitive fuzzy logic. This not only can restore the voltage/frequency deviations, but also optimize the trade-off between dynamic response and steady-state performance. Also, the restoration using the DG's own or neighboring information is fully explored, ensuring the plug-and-play capability.

3) A transient control factor is introduced for a mild and steady activation of secondary control. Under the cooperation of advanced MPC control and optimized distributed cooperative secondary control, the microgrid system is comprehensively investigated in a hierarchical view with a complete operational process and various case studies.

It should be noted that the proposed UMPVIC strategy and the distributed fuzzy cooperative algorithm fully comply with the microgrid's hierarchical control architecture [1],[2]. These two approaches work together to achieve an overall satisfactory performance of a microgrid. Specifically, the UMPVIC is implemented at the primary and tertiary layers to achieve load sharing and facilitate operation mode transition, while the distributed fuzzy cooperative algorithm is implemented at the secondary layer to restore the frequency and voltage.

The remainder of this paper is organized as follows. The microgrid hierarchical control framework is reviewed in Section II. The proposed UMPVIC strategy is presented in Section III. In Section IV, the distributed fuzzy cooperative secondary control is developed. The overall control strategy is illustrated in Section V. Case studies and discussion are presented in Section VI. Finally, conclusion is drawn in Section VII.

II. REVIEW OF HIERARCHICAL CONTROL FRAMEWORK

In microgrid hierarchical control architecture, each level has its own objective. Primary control stabilizes systemic frequency/voltage and shares power proportionally. Secondary control eliminates the inherent deviations brought by the primary control and prepares for grid connection. Tertiary control, the highest control level, is aimed to achieve interconnected power flows and maximize economic benefits under the grid-connected operation.

A. Primary Control

As the first and lowest control level inside the microgrid, the primary control aims at forming an islanded system for its own stable and sound operation. In order to achieve a proportional power sharing among DGs, the droop control method is used, which can be formulated as follows

$$f = f^* - mP \tag{1}$$

$$E = E^* - nQ \tag{2}$$

where f^* and E^* are the nominal network frequency and voltage, m and n the droop coefficients, P and Q the instantaneous measured active power and reactive power, respectively.

Thereafter, the droop control outputs f and E are synthesized for the usage of three phases with the following equation

$$\begin{cases} u_a = E\sin(2\pi f + 0) \\ u_b = E\sin(2\pi f - 2\pi/3) \\ u_c = E\sin(2\pi f + 2\pi/3) \end{cases} \tag{3}$$

In practical applications, the common abc reference frame is usually transferred into the $\alpha\beta$ stationary orthogonal reference frame through

$$u_{\alpha,\beta}^* = \frac{2}{3}[1 \ e^{(2\pi/3)j} \ e^{(4\pi/3)j}][u_a \ u_b \ u_c]^{\mathbf{T}} \tag{4}$$

After the voltage reference is determined by the droop controller, an inner voltage and current cascaded control loop is conventionally utilized to generate switching signals to control DG inverters [2], [3]. Alternatively, an inner MPC controller has

been recently reported by researchers to replace the conventional cascaded control loop [10], [11].

B. Secondary Control

In droop control, the increased load demand is met by reducing system frequency and voltage magnitudes. This principle inevitably causes deviations from the rated frequency and voltage. In order to mitigate these deviations, the so-called secondary control becomes a necessity.

To restore the frequency and voltage, secondary control principle is to shift the entire droop control curve along the vertical axis with an additional offset, which is expressed as

$$f = f^* - mP + \Delta f \tag{5}$$

$$E = E^* - nQ + \Delta E \tag{6}$$

where Δf and ΔE are frequency and voltage offsets. Traditionally, these offsets can be obtained by using centralized strategies that require central communication and computation units to collect and process the massive information of all DGs.

C. Tertiary Control

As the highest level in the hierarchy, tertiary control operates when the microgrid is connected to the main grid. As aforementioned, it deals with economic dispatching, operation scheduling, and power flow between the MG and main grid. Notice that tertiary control is also referred to the coordination of multiple microgrids interacting with one another in networked microgrids [1]. Economic dispatching is out of the scope of this study, Here, we focus on the quantitative and bidirectional power flows in tertiary control.

III. PROPOSED UMPVIC STRATEGY

DGs are the fundamental units that form a microgrid. In this section, an UMPVIC strategy is proposed for DGs operating in both islanded and grid-connected modes. The control diagram of the UMPVIC strategy is illustrated in Fig. 1, where a voltage source converter (VSC) is connected to the point of common coupling (PCC). In the figure, "A" and "B" are switches that operate simultaneously for both the circuit and algorithm. For example, "A" means disconnection from the main grid. Correspondingly equations (14) and (18) as the "islanded mode" algorithm should be used.
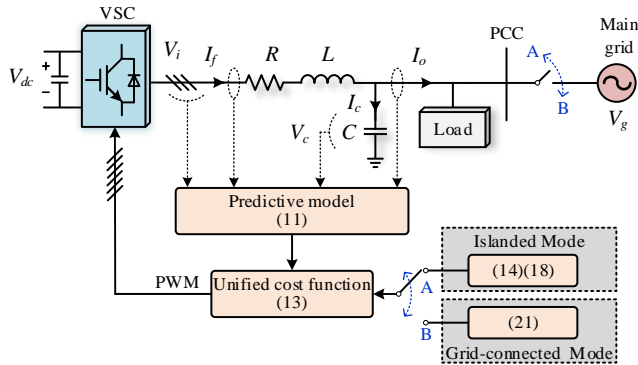

Fig. 1. Schematic diagram of the proposed UMPVIC strategy for VSCs.

A. DG Modeling

In this study, a two-level three-phase VSC is adopted for the power conversion. Depending on the VSC switching states, totally eight (2^3) output voltage vectors can be generated as

$$\begin{cases} i = 1, 2, ..., 6 : V_i = \dfrac{2}{3} V_{dc} e^{(i-1)(\pi/3)j} \\ i = 0, 7 : V_i = 0 \end{cases} \tag{7}$$

where V_{dc} is DC source voltage.

Essentially, the UMPVIC control principle is built upon the LC filter dynamics. According to Kirchhoffs Current Law (KCL) and Kirchhoffs Voltage Law (KVL), the following equations can be derived

$$C \frac{dV_c}{dt} = I_c = I_f - I_o \tag{8}$$

$$L \frac{dI_f}{dt} = V_i - I_f R - V_c \tag{9}$$

where V_c and I_c are the capacitor voltage and current, respectively; I_f and I_o are the inductor current and DG output current, respectively. (8) and (9) can then be further rewritten into a matrix form as

$$\dot{x} = Ax + Bu \tag{10}$$

where

$$x = \begin{bmatrix} V_c \\ I_f \end{bmatrix}, \quad u = \begin{bmatrix} V_i \\ I_o \end{bmatrix}, \quad A = \begin{bmatrix} 0 & 1/C \\ -1/L & -R/L \end{bmatrix}, \quad B = \begin{bmatrix} 0 & -1/C \\ 1/L & 0 \end{bmatrix}$$

Applying Euler forward discretization method, the following equation (also called predictive model) can be obtained

$$x(k+1) = e^{AT_s} x(k) + A^{-1}(e^{AT_s} - I_{2\times2}) Bu(k) \tag{11}$$

where $I_{2\times2}$ is the identity matrix. Employing (11), the DG output voltage V_c and inductor current I_f at next $(k+1)$th sampling instant can be predicted according to present k-instant states.

B. Cost Function Design of Islanded UMPVIC

In the majority of existing relevant studies [13-15, 24, 25], in order to provide a stable voltage supply, only voltage magnitude is formulated in the cost function as

$$J_V = (V_{c\alpha,\beta}^* - V_{c\alpha,\beta}(k+1))^2 \tag{12}$$

where V_c^* is capacitor voltage reference, subscript α or β means the sub-variable on coordinate in the stationary orthogonal reference frame. However, after careful observation of (11), which is derived from (8) and (9), one can find an interesting mathematical relationship. That is, the VSC output voltage V_i that directly impacts the DG performance is not explicitly involved in capacitor voltage prediction. By contrast, V_i is needed for inductor current prediction. This means $I_f(k+1)$ is strongly linked to V_i. Inspired by this, the cost function (12) can be re-designed by formulating not only the capacitor voltage but also the inductor current as

$$J_{VI} = (V_{c\alpha,\beta}^* - V_{c\alpha,\beta}(k+1))^2 + (I_{f\alpha,\beta}^* - I_{f\alpha,\beta}(k+1))^2 \tag{13}$$

where I_f^* is the inductor current reference. By including the current term in the cost function, the original control objective, i.e., the capacitor voltage or DG output voltage, can be better regulated.

In (13), $V_{c\alpha,\beta}(k+1)$ and $I_{f\alpha,\beta}(k+1)$ can be obtained from (11). Then the next step is to determine the two references $V_{c\alpha,\beta}^*$ and $I_{f\alpha,\beta}^*$. In a single VSC system, obviously, $V_{c\alpha,\beta}^*$ can be set as an ideal sinusoidal wave for voltage supply [24]. In microgrids with parallel VSCs coordinated by droop method, $V_{c\alpha,\beta}^*$ should be determined from the droop controller as

$$V_{c\alpha,\beta}^* = u_{\alpha,\beta}^* \qquad (14)$$

where $u_{\alpha,\beta}^*$ is the voltage reference from the droop controller, as illustrated previously in Section II. As for $I_{f\alpha,\beta}^*$, it can be obtained by applying KCL as

$$I_{f\alpha,\beta}^* = I_{c\alpha,\beta}^* + I_{o\alpha,\beta}^* \qquad (15)$$

Meanwhile, $V_{c\alpha,\beta}^*$ can be expressed as

$$V_{c\alpha,\beta}^* = V_{c\alpha}^* + jV_{c\beta}^* = |V_c^*|\cos(\omega t) + j|V_c^*|\sin(\omega t) \qquad (16)$$

where $|V_c^*|$ is the voltage magnitude. Using (16) and (8), also assuming DG output current I_o is unchanged during an inter-sampling time period, one can obtain

$$\begin{cases} I_{c\alpha,\beta}^* = C\dfrac{dV_{c\alpha}^*}{dt} + jC\dfrac{dV_{c\beta}^*}{dt} = -\omega CV_{c\beta}^* + j\omega CV_{c\alpha}^* \\ I_{o\alpha,\beta}^* = I_{o\alpha,\beta} \end{cases} \qquad (17)$$

Subsequently, substituting (17) into (15), the inductor current reference can eventually be obtained as

$$I_{f\alpha,\beta}^* = -\omega CV_{c\beta}^* + j\omega CV_{c\alpha}^* + I_{o\alpha,\beta} \qquad (18)$$

C. Cost Function Design of Grid-connected UMPVIC

Unlike islanded mode, grid-connected microgrids can get both frequency and voltage supports from the main grid. Thus a different control method is needed. In this case, the PCC voltage is strongly fixed by the main grid as $V_g = V_{pcc} \approx V_c$. Since the LC filter is maintained when operation mode changes, equations (8) and (9) are still feasible, which means both $V_c(k+1)$ and $I_f(k+1)$ can still be predicted from (11). Now, the control method design for the grid-connected mode only relies on constructing a suitable cost function with the goal of bidirectional power flow.

The active power and reactive power are calculated by

$$\begin{cases} P = \dfrac{3}{2}(V_{c\alpha}I_{o\alpha} + V_{c\beta}I_{o\beta}) \\ Q = \dfrac{3}{2}(V_{c\beta}I_{o\alpha} - V_{c\alpha}I_{o\beta}) \end{cases} \qquad (19)$$

In conventional MPC of grid-connected inverters, the active and reactive powers are regulated in the form as

$$J_{PQ} = (P^* - P(k+1))^2 + (Q^* - Q(k+1))^2 \qquad (20)$$

where P^* and Q^* are the power references; $P(k+1)$ and $Q(k+1)$ are the powers predicted either from the derivative on the calculation of instantaneous P and Q [14] using (19), or from the real and imaginary part of the product of $V_c(k)$ and $I_f(k+1)$ [26].

Under this circumstance, when the microgrid changes operation modes, the cost function will alter accordingly between (13) and (20). However, this kind of alteration makes the cost function design neither straightforward nor reliable. In light of this, instead of using (20), the cost function in grid-connected operation can actually be formulated into to a unified form as (13) in islanded operation. The key is to explore a link between the power and the voltage and current. This process can be realized by the following transformation

$$\begin{cases} V_{c\alpha,\beta}^* = V_{g\alpha,\beta} \\ I_{f\alpha}^* = \dfrac{2}{3}\left(\dfrac{P^* V_{c\alpha}^* + Q^* V_{c\beta}^*}{V_{c\alpha}^{*2} + V_{c\beta}^{*2}}\right) \\ I_{f\beta}^* = \dfrac{2}{3}\left(\dfrac{P^* V_{c\beta}^* - Q^* V_{c\alpha}^*}{V_{c\alpha}^{*2} + V_{c\beta}^{*2}}\right) \end{cases} \qquad (21)$$

Here, $V_{g\alpha,\beta}$ is the actual grid voltage that guides the converter output voltage to track the referenced grid voltage.

IV. DISTRIBUTED FUZZY COOPERATIVE SECONDARY CONTROL

Centralized secondary control requires a central controller and a heavy communication burden, which suffers from the single point of failure problem and hence, degrades system reliability. In this study, an optimal distributed fuzzy cooperative secondary control is developed. In graph theory, a microgrid can be expressed as a digraph $\vartheta = (\upsilon, \varepsilon, A)$, where the DGs are denoted as nodes or agents $\upsilon = \{v_1, v_2, ..., v_N\}$. Their communication connections are denoted as edges $\varepsilon \subset \upsilon \times \upsilon$. If node j sends data to adjacent node i, this edge can be described as $(v_j, v_i) \in \varepsilon$, and its corresponding weight becomes $a_{ij} = 1$, otherwise $a_{ij} = 0$. The set of a_{ij} is called adjacency matrix $A = [a_{ij}]_{N \times N}$. Obviously, this adjacency matrix A encodes the communication pattern among DGs.

The distributed cooperative control seeks to realize a tracking synchronization among DGs based on the system dynamics. In microgrid secondary control, it aims to regulate the system frequency and DGs output voltage to reach consensus. To derive the control protocol, input-output feedback linearization [17, 18] is applied on (1) and (2) for DG$_i$.

$$\dot{f_i} = \Delta\dot{f_i} - m_i\dot{P_i} \equiv u_{fi} = e_{fi}d_f \qquad (22)$$

$$\dot{E_i} = \Delta\dot{E_i} - n_i\dot{Q_i} \equiv u_{Ei} = e_{Vi}d_v \qquad (23)$$

In (22), since the system frequency is a global variable in steady state, it can have the similar linearization operation as

$$m_i\dot{P_i} \equiv u_{pi} = m_i \cdot (P_i \cdot \dfrac{1}{\omega_c s + 1} - P_i) \cdot d_p \qquad (24)$$

While for (23), it accordingly has

$$\dot{Q_i} = \dfrac{1}{\omega_c} \cdot (Q_i - Q_i \cdot \dfrac{1}{\omega_c s + 1}) \qquad (25)$$

In the above (22)-(25), $\cdot$ is differential operation; ω_c is filtering parameter that is the derivative of the low-pass filter cut-off frequency; d_p, d_f, d_v are the secondary control coefficients; e_{fi} and e_{vi} are the tracking errors by using DG's own information or its neighboring information as

$$e_{fi} = \sum_{j \in N_i} a_{ij}(f_j - f_i) + g_i(f^* - f_i) \qquad (26)$$

$$e_{vi} = \sum_{j \in N_i} a_{ij}(V_{cj} - V_{ci}) + g_i(V_c^* - V_i) \qquad (27)$$

where g_i is the pinning gain indicating whether the DG can access the constant frequency/voltage reference.

Then, the control protocol of distributed cooperative secondary control can be described as follows

1) for secondary frequency control

$$\Delta f_i = (u_{fi} + u_{pi}) \cdot \dfrac{1}{s} \qquad (28)$$

2) for secondary voltage control

$$\Delta E_i = (n_i \dot{Q}_i + u_{Ei}) \cdot \frac{1}{s} \qquad (29)$$

In order to avoid complex and time-consuming tuning of coefficients d_p, d_f and d_v, and to increase the adaptability and flexibility of cooperative action, a fuzzy control of selecting suitable coefficients is utilized. The fuzzy control uses fuzzy logic to reflect human thinking and operating experience, transforming nonlinear and complex control algorithms or models to simple fuzzy rules [27, 28].

The fuzzy controller design generally includes the following steps [29]:

1) Fuzzification: to transform input variables to fuzzy variable sets that obey membership functions;

2) Fuzzy inference: to determine inferential results based on the predefined "if…then" fuzzy rules;

3) Defuzzification: as an inverse process of fuzzification, to translate fuzzy inference results into output control variables (coefficients d_p, d_f and d_v).

Moreover, for a smooth activation of the secondary control, a transient control ramp function is introduced, which is expressed as

$$y = x - t$$
$$t \le x \le t+1; 0 \le y \le 1 \qquad (30)$$

where t indicates the instant when secondary control activates. It is only triggered when secondary control is switched on. The output of this ramp function y will then be multiplied by the secondary control outputs Δf_i and ΔE_i, respectively. Once the secondary control is activated, y increases linearly from 0 to 1 within one second. In this way, the frequency and voltage compensation from the secondary controller will be added to the primary droop controller gradually to avoid overshoot and system instability.

The control diagram of the proposed distributed fuzzy cooperative secondary control is illustrated in Fig. 2. *abs* means the absolute operator, which locates in front of fuzzy controllers. The coefficients d_p, d_f and d_v (in dashed line) are replaced by fuzzy controllers, which is simple and straightforward without significantly changing the control architecture. The transient control ramp function is depicted in the blue dash block.
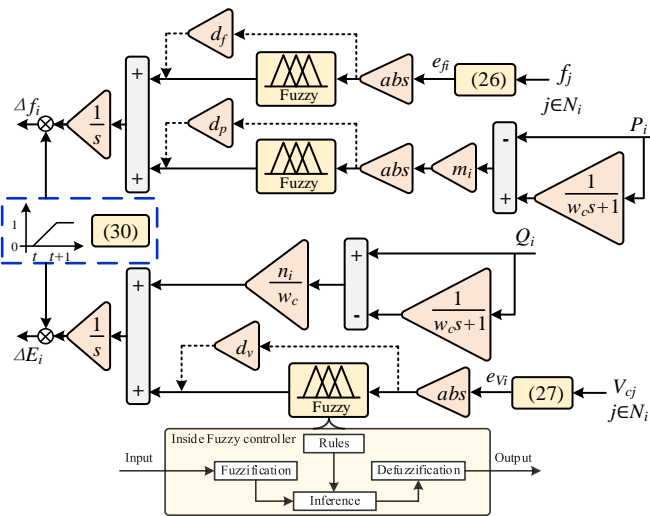

Fig. 2. Block diagram of the proposed distributed fuzzy cooperative secondary control

V. OVERALL CONTROL ARCHITECTURE

For better illustration, Fig. 3 depicts the overall control strategy in this paper from the perspective of hierarchical architecture. The proposed UMPVIC strategy is mainly involved in the primary and tertiary control levels. At primary control layer in islanded operation, it is cooperated with droop method to achieve load sharing among DGs. Meanwhile, the proposed fuzzy optimized distributed cooperative control is implemented on the secondary level. It aims to generate a compensation for the primary droop controller in order to eliminate the voltage and frequency deviations. The DGs exchange information with their neighbors based on a sparse communication network with the purpose of improving control reliability. At tertiary control layer, the fuzzy optimized distributed cooperative control is deactivated and grid-connected operation begins. In this case, active power and reactive power can both be regulated independently and quantitatively, which enables flexible and bidirectional power exchange with the main grid. Bidirectional power flow between microgrids and utility grid is an interesting topic. Although it is out of the scope of this paper, it is worth mentioning that the power exchanges should be determined according to various aspects such as electricity prices, power transmission losses, operational benefits, etc. [30]
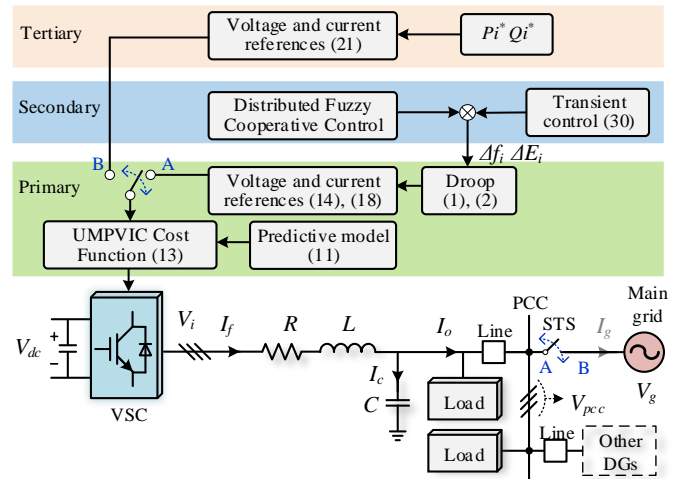

Fig. 3. The overall control architecture
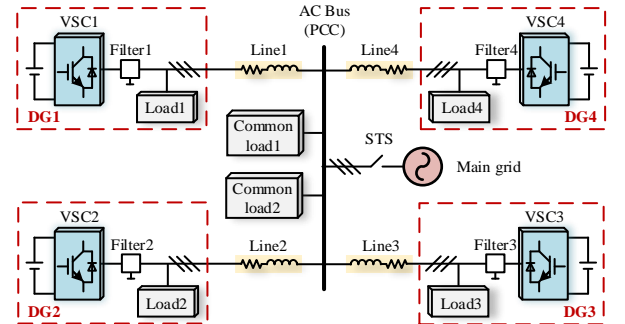
VI. VERIFICATION

Fig. 4. Microgrid configuration with multiple VSCs

The proposed control strategy is validated through case studies. A microgrid with four DGs is built in MATLAB Simscape Power Systems environment, as shown in Fig. 4. The AC bus is denoted as the point of common coupling (PCC) where the main grid can

be interfaced through a static transfer switch (STS). The system and control parameters are listed in Table I. The default values of the graph structure of DG communication are listed in the table. The setting of the fuzzy controller is also given in the table. Here, we use "mamdani" method for the inference, which has been widely recognized and used in fuzzy control domain [31].

TABLE I. System and Control Parameters

Description	Value
DG capacity	120kW (default value)
DC rated voltage	1kV
AC rated voltage	0.38kV (p-p, rms), 50Hz
AC-bus LC filter	$R = 20m\Omega$, $L = 3.6mH$, $C = 0.2mF$
Line impedance	$R = 0.1\Omega$, $L = 2.4mH$
Droop coefficient	$m = 1e-5$, $n = 2.5e-4$ (default value)
Filtering parameter	$\omega_c = 0.16$
Sampling interval	40µs
Prediction horizon	$N=1$ with one-step delay compensation
Local load 1-4	(10kW, 0kVar)
Common load 1-2	(40kW, 0kVar)
Secondary control	
Graph structure	$a_{ij} = 0$, $g_i = 1$ (default values)
Fuzzy control	
For d_f, d_p, d_v input	Range = [0,0.2], [0,0.04], [0 1.2] respectively; there are 8 membership functions that are all "Gaussian Function" and uniformly distributed (named: in1, in2, …, in8)
For d_f, d_p, d_v output	Ranges are all [2,50]; there are 8 membership functions which are all "Gaussian Function" and uniformly distributed (named: out1, out2, …, out8)
Inference method	"Mamdani" method [31]
Rules	If in1 then out1, If in2 then out2, …, If in8 then out8

A. Primary Control

In the first scenario, only primary control is implemented under islanded operation. Initially all local loads and common load #1 are connected. Fig. 5 compares the performance of traditional method and the proposed UMPVIC scheme. As shown, the harmonic spectrum of the proposed method is clearer than traditional method, particularly around 2.2kHz. Thus, the THD of the proposed primary control is 1.49%, whereas the traditional control leads to a THD of 1.66% under the same circumstance. This is because the proposed UMPVIC scheme fully considers the LC filter's dynamics and includes inductor current in the cost function, resulting a better voltage supply quality. 1.49% is smaller than 1.5% that is the voltage distortion limit as specified by IEEE Std 519-2014. Thus, a high-quality voltage supply is provided.
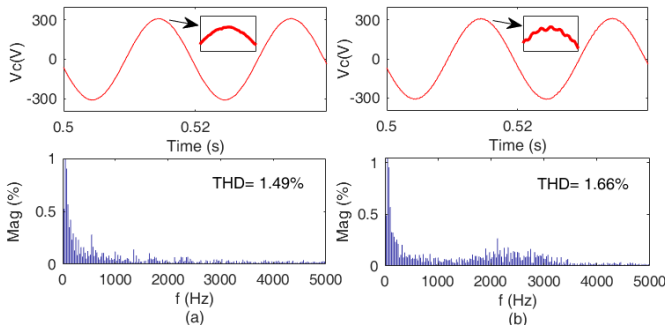

Fig. 5. Voltage quality comparison. (a) proposed UMPVIC strategy, (b) traditional method

Then, the microgrid performance under load changes by using the proposed UMPVIC strategy is studied. Common load #2 is switched in at 1s and switched out at 3s. As shown in Fig. 6, the powers among DGs can be properly shared to meet the load demand. However, due to the nature of droop method, the frequencies and voltages are both deviated from nominal levels, particularly when the load increases. Considering all DGs, the highest frequency deviation error in Fig. 6 (c) is 0.2941Hz, while the highest voltage deviation error in Fig. 6 (d) is 1.4865V. To address the voltage and frequency deviations, secondary control will be implemented in the next test.
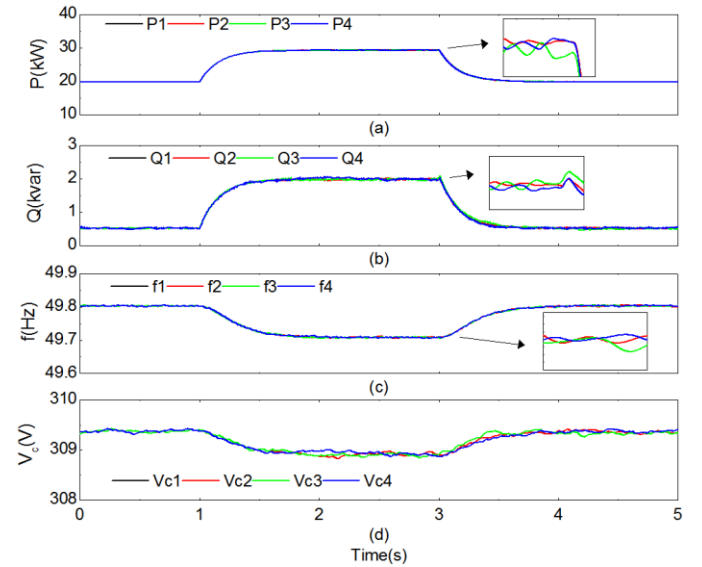

Fig. 6. Islanded operation of proposed UMPVIC strategy when load changes

B. Secondary Control

In this test, the proposed distributed fuzzy cooperative secondary control is utilized. The results are shown in Fig. 7. When compared to Fig. 6 without using the secondary control, it can be observed that the system frequency and DG output voltage are now tightly maintained at their nominal values, especially for the voltage control. At 1s and 3s during load variations, the proposed control can rapidly restore the trajectories back to the original steady points.
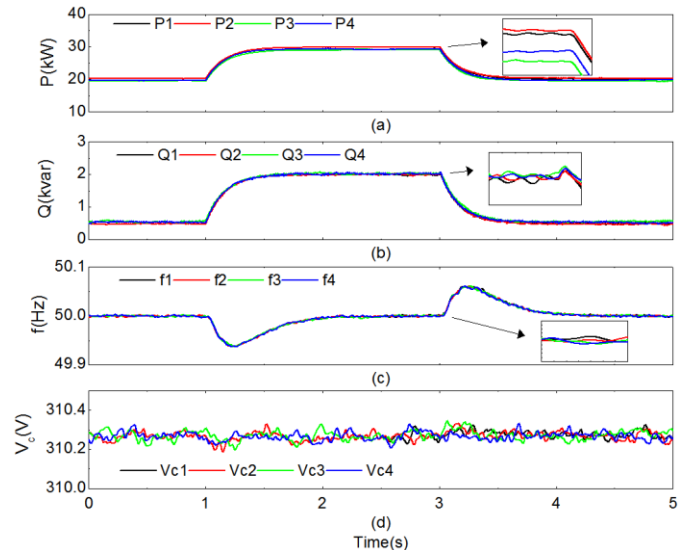

Fig. 7. Islanded operation of proposed UMPVIC strategy with distributed fuzzy

To further demonstrate the effectiveness of the optimal fuzzy cooperative secondary control, it has been compared with the traditional secondary control with fixed secondary coefficients d_p, d_f and d_v. Fig. 8 shows the comparison in terms of frequency performance. It can be seen that smaller coefficients ($d_p=d_f=d_v=2$) result in a slower response but with fewer oscillations. In contrast, larger coefficients ($d_p=d_f=d_v=50$) lead to a faster response but with more oscillations or "spikes". These frequency spikes are not wanted in power system. For example, they will cause large electromagnetic torque oscillations in motor loads, resulting in an inefficient operation and a gradual breakdown. On the other hand, the proposed distributed fuzzy cooperative secondary control can achieve a better trade-off between the response and oscillations. Fig. 9 presents the corresponding coefficients inside the fuzzy controller of DG1. These reveal that, instead of being maintained constant, the coefficients are dynamically adjusted according to the preset fuzzy logic for optimization.
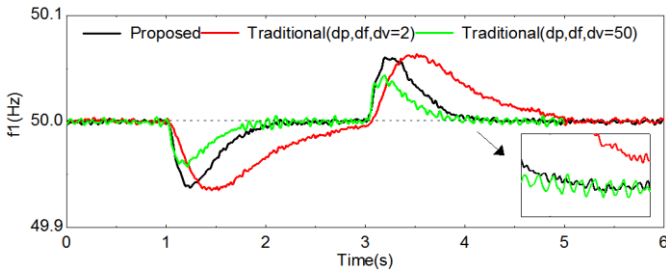

Fig. 8. Comparison between the proposed distributed fuzzy cooperative secondary control and traditional secondary control.
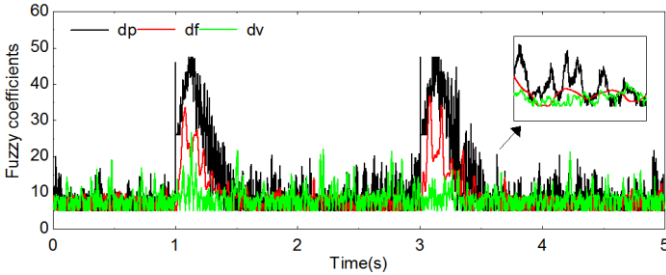

Fig. 9. Coefficient optimization inside the fuzzy controller.

C. Tertiary Control

In the third scenario, the STS switches on at 1s and grid-connected mode is activated with active power exchange demand at 10kW. At the same time, the secondary control is deactivated because the system is ready to get the strong support from the main grid. As can be seen in Fig. 10, the system turns into the grid-connected mode from the islanded mode smoothly. The active power tracks tightly to the reference, and the frequency is also kept stable at the nominal value. At 3s, the STS switches off and the microgrid translates back to islanded mode.
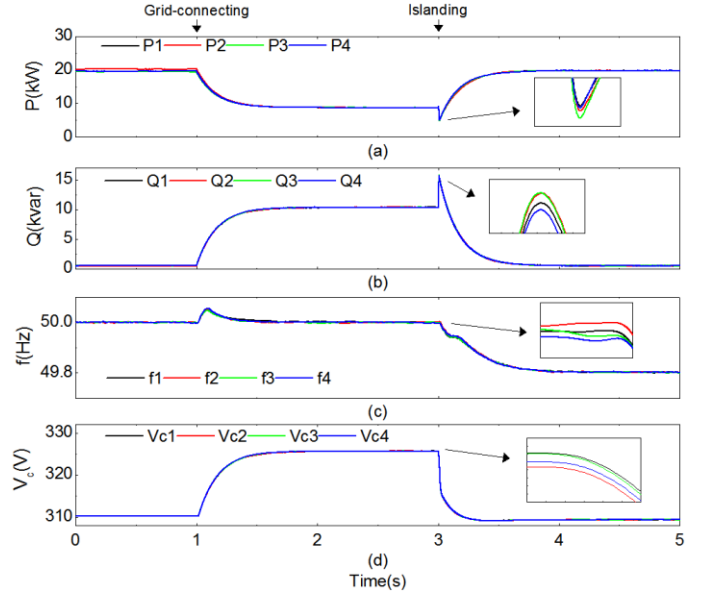

Fig. 10. Grid-connecting and islanding test

D. Distributed Cooperative Performance

Here, the communication network is changed to Fig. 11 for the evaluation of DGs' secondary cooperative control under islanded operation. The same load variation pattern as Subsection-A is adopted here. In this case, only DG1 can access the frequency and voltage references, while other DGs can get their own and neighboring instantaneous frequency and voltage information. Based on this graph structure, the adjacency matrix and the pinning gain become

$$\begin{cases} A = [a_{ij}]_{4\times4} = \begin{bmatrix} 0 & 0 & 0 & 0 \\ 1 & 0 & 0 & 0 \\ 0 & 1 & 0 & 0 \\ 0 & 0 & 1 & 0 \end{bmatrix} \\ [g_i] = [1 \quad 0 \quad 0 \quad 0] \end{cases} \qquad (31)$$
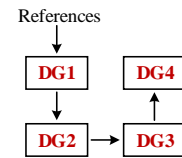

Fig. 11. Directed communication graph from DG 1 to DG4

Fig. 12 presents the distributed cooperative performance. As shown, the system can restore the frequency and voltage as well as maintain their stabilization when load changes. Notice that the deviated and oscillated degrees during the transient process are increasing slightly from DG1 to DG4. This is because the distorted information sent by adjacent DGs has been accumulated along the directed communication path, as illustrated in Fig. 11. This accumulated effect depends on the communication topology and connectivity. Though out of the scope of this work, we want to point out that topology optimization of data communication network is an interesting and important research area as it can affect DGs performance in microgrids.
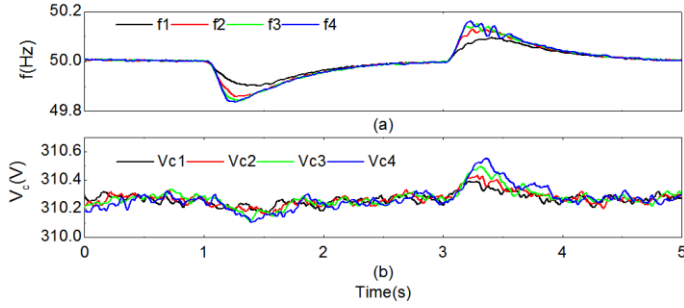
Fig. 12. Distributed cooperative performance with directed communication graph from DG 1 to DG4.

E. Plug-and-Play Capability

The plug-and-play capability of the proposed strategy is demonstrated in this test. Initially, four local loads and one common load are connected. At 1s, assuming there is a fault (e.g., short circuit, open circuit or the malfunctions of circuit breaker and protective relays) in DG4, it is disconnected from the microgrid. Then at 3s, DG4 is connected back upon fault clearance. Further, DG2 and DG3 are both disconnected at 5s and reconnected at 7s. The plug-and-play performance is presented in Fig. 13. From Fig. 13 (a) and (b), it can be seen that when DG4, DG2 and DG3 are switched off at different time instants, the rest of DGs immediately pick up the power demand and share the load. Then, once DG4, DG2 and DG3 are plugged into the microgrid, the operating DGs share the system power accordingly. During the whole process, the system frequency and DG output voltage can be maintained at the nominal values, as shown in Fig. 13 (c) and (d). Here, it is worth mentioning that the disconnected DGs can continue to power their local loads when they are switched off from the microgrid. This is another attractive merit of the proposed strategy.
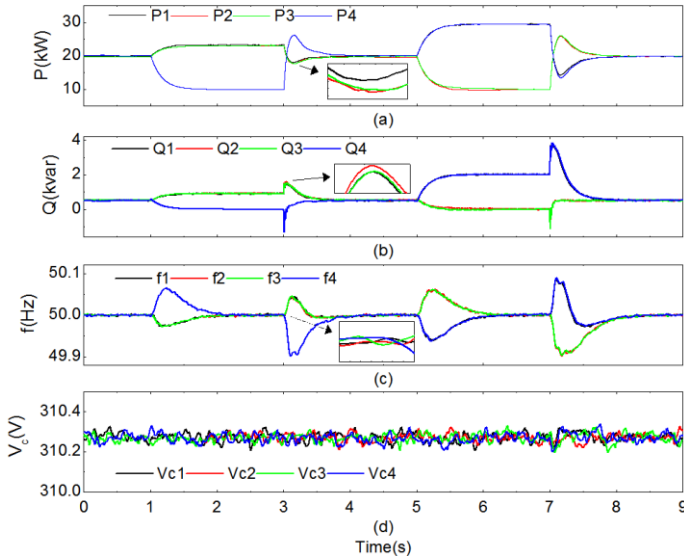

Fig. 13. Plug-and-play performance

F. DGs with unequal power generations

Here, different DG capacities (DG1:80kW, DG2:100kW, DG3:120kW, DG4:140kW) are tested, while the same load profile in Fig. 6 is applied. The performance in islanded mode is shown in Fig. 14. From Fig. 14 (a) and (b), it can be seen that the powers are shared proportionally to their capacities. Fig. 14 (c) and (d) are the results of the system performance without

secondary control. Since the frequency is a global variable, their frequencies are the same in steady state, whereas the voltages present obvious drops. Fig. 14 (e) and (f) show the results of the system performance with the proposed distributed secondary control. It can be observed that, under unequal DG power generations, the frequencies and voltages are maintained at their rated values.
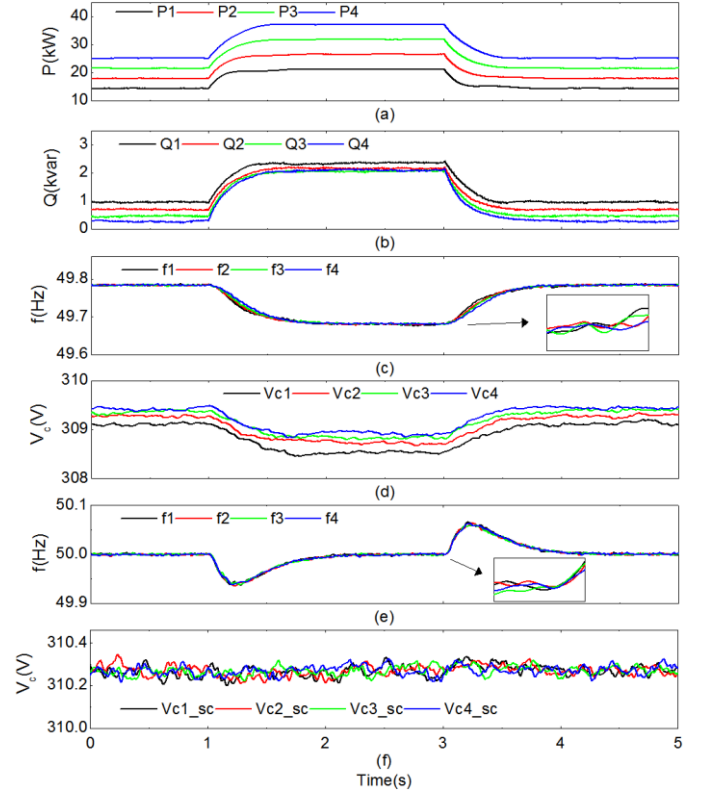

Fig. 14. Islanded operation of proposed UMPVIC and distributed fuzzy cooperative secondary control strategy with different DG capacities

G. Comparisons with recent relevant literature

In this paper, we have proposed two new control mechanisms that are different from the existing control methods for microgrid multi-mode operations. The first one is the unified UMPVIC, which forms a unified predictive model and cost function, taking into account both voltage and current factors without altering the control architecture. Hence, an improved voltage supply and bidirectional power flow are achieved. This is different from recent relevant studies [32-35], which neither achieve a unified control architecture nor consider the changing trend of capacitor voltage (i.e., the inductor current). The second one is the fuzzy optimized distributed cooperative control, which can dynamically regulate the secondary coefficients in an explicit and intuitive way. Thus, a trade-off between dynamic response and steady-state performance can be mitigated. To our best acknowledge, this self-adaptive mechanism has not been reported in recent distributed cooperative control [36-38].

VII. CONCLUSIONS

In this work, a microgrid with four DGs in a hierarchical control architecture is studied. A unified model predictive voltage and current control (UMPVIC) strategy is proposed for both islanded and grid-connected operations and their smooth transition. The cost function is formulated in a unified form by considering DG voltage and current. As a result, different

operation modes can be achieved without altering the control architecture. The proposed UMPVIC strategy can be flexibly used in primary control layer for proper load sharing and in tertiary control layer for bidirectional power flow. Furthermore, by only using DGs' own and neighboring information, a distributed fuzzy cooperative algorithm is developed at the secondary control level to mitigate the voltage and frequency deviations inherent from the primary droop layer. The fuzzy controller can optimize the secondary control coefficients for further voltage quality improvement. Comprehensive tests under various scenarios including load variations and plug-and-play operation demonstrate the advantages of the proposed control strategy over traditional methods.

However, the following points should be noticed:

1) Compared to the traditional cascaded control structure, more system information (e.g., predictive model, cost function, alternative voltage vectors and solving process) is needed. Thus, computational burden will increase for local DG controllers.

2) The switching frequency of the proposed MPC scheme for power converter control is not constant, which brings in difficulties in LC filter design.

3) Since the distributed secondary control is performed on a sparse communication network, a two-way data exchange mechanism is needed among DGs.

REFERENCES

[1] A. Mohammed, S. S. Refaat, S. Bayhan, and H. Abu-Rub, "AC Microgrid Control and Management Strategies: Evaluation and Review," *IEEE Power Electron. Mag.*, vol. 6, no. 2, pp. 18–31, 2019.

[2] J. M. Guerrero, J. C. Vasquez, J. Matas, L. G. de Vicuna and M. Castilla, "Hierarchical Control of Droop-Controlled AC and DC Microgrids—A General Approach Toward Standardization," *IEEE Trans. Ind. Electron.*, vol. 58, no. 1, pp. 158-172, Jan. 2011.

[3] J. C. Vasquez, J. M. Guerrero, A. Luna, P. Rodriguez and R. Teodorescu, "Adaptive Droop Control Applied to Voltage-Source Inverters Operating in Grid-Connected and Islanded Modes," *IEEE Trans. Ind. Electron.*, vol. 56, no. 10, pp. 4088-4096, Oct. 2009.

[4] T. L. Vandoorn, B. Meersman, J. D. M. De Kooning and L. Vandevelde, "Transition From Islanded to Grid-Connected Mode of Microgrids With Voltage-Based Droop Control," *IEEE Trans. Power Syst.*, vol. 28, no. 3, pp. 2545-2553, Aug. 2013.

[5] S. Bayhan and H. Abu-Rub, "A Simple Control Technique for Distributed Generations in Grid-Connected and Islanded Modes," *2018 IEEE 27th International Symposium on Industrial Electronics (ISIE)*, Cairns, QLD, 2018, pp. 1237-1242.

[6] T. Tran, T. Chun, H. Lee, H. Kim and E. Nho, "PLL-Based Seamless Transfer Control Between Grid-Connected and Islanding Modes in Grid-Connected Inverters," *IEEE Trans. Power Electron.*, vol. 29, no. 10, pp. 5218-5228, Oct. 2014.

[7] Z. Yi, W. Dong and A. H. Etemadi, "A Unified Control and Power Management Scheme for PV-Battery-Based Hybrid Microgrids for Both Grid-Connected and Islanded Modes," *IEEE Trans. Smart Grid*, vol. 9, no. 6, pp. 5975-5985, Nov. 2018.

[8] M. Karimi-Ghartemani, P. Piya, M. Ebrahimi, and S. A. Khajehoddin, "A universal controller for grid-connected and autonomous operation of three-phase dc/ac converters," in *Proc. 2015 IEEE Energy Convers. Congr. Expo.*, 2015, pp. 1666–1673.

[9] X. Hou *et al.*, "Distributed Hierarchical Control of AC Microgrid Operating in Grid-Connected, Islanded and Their Transition Modes," *IEEE Access*, vol. 6, pp. 77388-77401, 2018.

[10] T. Dragičević, "Model Predictive Control of Power Converters for Robust and Fast Operation of AC Microgrids," *IEEE Trans. Power Electron.*, vol. 33, no. 7, pp. 6304-6317, Jul. 2018.

[11] Y. Shan and *et al*, "A Model Predictive Control for Renewable Energy Based AC Microgrids Without Any PID Regulators," *IEEE Trans. Power Electron.*, vol. 33, no. 11, pp. 9122-9126, Nov. 2018.

[12] R. Heydari, M. Gheisarnejad, M. H. Khooban, T. Dragicevic and F. Blaabjerg, "Robust and Fast Voltage-Source-Converter (VSC) Control for Naval Shipboard Microgrids," *IEEE Trans. Power Electron.*, vol. 34, no. 9, pp. 8299-8303, Sept. 2019.

[13] X. Li, H. Zhang, M. B. Shadmand and R. S. Balog, "Model Predictive Control of a Voltage-Source Inverter With Seamless Transition Between Islanded and Grid-Connected Operations," *IEEE Trans. Ind. Electron.*, vol. 64, no. 10, pp. 7906-7918, Oct. 2017.

[14] A. J. Babqi and A. H. Etemadi, "MPC-based microgrid control with supplementary fault current limitation and smooth transition mechanisms," *IET Generation, Transmiss. Distrib.*, vol. 11, no. 9, pp. 2164-2172, Jun. 2017.

[15] M. Jayachandran, G. Ravi. "Decentralized model predictive hierarchical control strategy for islanded AC microgrids," *Electr. Power Syst. Res.*, vol.170, pp. 92-100, May 2019.

[16] Y. Xu, H. Sun, W. Gu, Y. Xu, and Z. Li, "Optimal Distributed Control for Secondary Frequency and Voltage Regulation in an Islanded Microgrid," *IEEE Trans. Ind. Inform.*, vol. 15, no. 1, pp. 225–235, 2019.

[17] A. Bidram, A. Davoudi, F. L. Lewis, and Z. Qu, "Secondary control of microgrids based on distributed cooperative control of multi-agent systems," *IET Gener. Transm. Distrib.*, vol. 7, no. 8, pp. 822–831, 2013.

[18] A. Bidram, A. Davoudi, F. L. Lewis, and J. M. Guerrero, "Distributed cooperative secondary control of microgrids using feedback linearization," *IEEE Trans. Power Syst.*, vol. 28, no. 3, pp. 3462–3470, 2013.

[19] N. M. Dehkordi, N. Sadati, and M. Hamzeh, "Fully Distributed Cooperative Secondary Frequency and Voltage Control of Islanded Microgrids," *IEEE Trans. Energy Convers.*, vol. 32, no. 2, pp. 675–685, 2017.

[20] X. Wu, C. Shen, and R. Iravani, "A Distributed, Cooperative Frequency and Voltage Control for Microgrids," *IEEE Trans. Smart Grid*, vol. 9, no. 4, pp. 2764–2776, 2018.

[21] Y. Xu, et al, "Optimal distributed control for secondary frequency and voltage regulation in an islanded microgrid," *IEEE Trans. Ind. Inform.*, vol. 15, no. 1, pp. 225–235, 2019.

[22] Y. Xu, Q. Guo, H. Sun, and Z. Fei, "Distributed Discrete Robust Secondary Cooperative Control for Islanded Microgrids," *IEEE Trans. Smart Grid*, vol. 10, no. 4, pp. 3620–3629, 2019.

[23] X. Wu *et al.*, "A Two-Layer Distributed Cooperative Control Method for Islanded Networked Microgrid Systems," *IEEE Trans. Smart Grid*, vol. 11, no. 2, pp. 942–957, 2020.

[24] P. Cortes, G. Ortiz, J. I. Yuz, J. Rodriguez, S. Vazquez and L. G. Franquelo, "Model Predictive Control of an Inverter With Output LC Filter for UPS Applications," *IEEE Trans. Ind. Electron.*, vol. 56, no. 6, pp. 1875-1883, Jun. 2009.

[25] J. Rodriguez et al., "State of the Art of Finite Control Set Model Predictive Control in Power Electronics," *IEEE Trans. Ind. Inform.*, vol. 9, no. 2, pp. 1003-1016, May 2013.

[26] P. Cortes, J. Rodriguez, P. Antoniewicz and M. Kazmierkowski, "Direct Power Control of an AFE Using Predictive Control," *IEEE Trans. Power Electron.*, vol. 23, no. 5, pp. 2516-2523, Sep. 2008.

[27] C. Andalib-Bin-Karim, X. Liang, and H. Zhang, "Fuzzy-Secondary-Controller-Based Virtual Synchronous Generator Control Scheme for Interfacing Inverters of Renewable Distributed Generation in Microgrids," *IEEE Trans. Ind. Appl.*, vol. 54, no. 2, pp. 1047–1061, 2018.

[28] R. V. A. Neves, R. Q. Machado, V. A. Oliveira, X. Wang, and F. Blaabjerg, "Multitask Fuzzy Secondary Controller for AC Microgrid Operating in Stand-alone and Grid-tied Mode," *IEEE Trans. Smart Grid*, vol. 10, no. 5, pp. 5640–5649, 2019.

[29] L. Foulloy, R. Boukezzoula, and S. Galichet, "An educational tool for fuzzy control," *IEEE Trans. Fuzzy Syst.*, vol. 14, no. 2, pp. 217–221, 2006.

[30] M. N. Alam, S. Chakrabarti and A. Ghosh, "Networked microgrids: state-of-the-art and future perspectives," *IEEE Trans. Ind. Inform.*, vol. 15, no. 3, pp. 1238–1250, 2019.

[31] Mamdani and Sugeno Fuzzy Inference Systems, MathWorks, https://ww2.mathworks.cn/help/fuzzy/types-of-fuzzy-inference-systems.html

[32] S. Bayhan and H. Abu-Rub, "Model Predictive Control Based Dual-Mode Controller for Multi-Source DC Microgrid," in *IEEE International Symposium on Industrial Electronics*, 2019, vol. 2019-June, pp. 908–913.

[33] I. Poonahela, S. Bayhan, H. Abu-Rub, and M. Begovic, "Implementation of Finite Control State Model Predictive Control with Multiple Distributed Generators in AC Microgrids," in *Proceedings - 2020 IEEE 14th International Conference on Compatibility, Power Electronics and Power Engineering, CPE-POWERENG 2020*, 2020, pp. 206–211.

[34] J. Hu and et al, "Model predictive control of microgrids – An overview," *Renew. Sustain. Energy Rev.*, vol. 136, 2021.

[35] F. Martinez, T. Morel, H. Fretes, J. Rodas, Y. Kali, and R. Gregor, "Model predictive current control of dual-mode voltage source inverter operations: Islanded and grid-connected," in *2020 5th International Conference on Renewable Energies for Developing Countries, REDEC 2020*, 2020.

[36] J. Lai, X. Lu, X. Yu, W. Yao, J. Wen, and S. Cheng, "Distributed multi-DER cooperative control for master-slave-organized microgrid networks with limited communication bandwidth," *IEEE Trans. Ind. Inform.*, vol. 15, no. 6, pp. 3443–3456, 2019.

[37] J. Zhang, X. Wang, and L. Ma, "A Finite-time Distributed Cooperative Control Approach for Microgrids," *CSEE J. Power Energy Syst.*, 2020.

[38] C. Dou, Y. Li, D. Yue, Z. Zhang, and B. Zhang, "Distributed cooperative control method based on network topology optimisation in microgrid cluster," *IET Renew. Power Gener.*, vol. 14, no. 5, pp. 939–947, 2020.

Yinghao Shan received his Ph.D. degree in Electrical Engineering from The Hong Kong Polytechnic University, Hong Kong, in 2020. Currently, he is a lecturer with the College of Information Science and Technology, Donghua University, Shanghai, China. His research interests include microgrids, predictive control and intelligent control.

Jiefeng Hu (S'12–M'14–SM'16) received the Ph.D. degree in electrical engineering from University of Technology Sydney, Australia, in 2013. He participated in the research of minigrids in Commonwealth Scientific and Industrial Research Organization, Newcastle, Australia. He was an Assistant Professor at The Hong Kong Polytechnic University, Hong Kong. Currently he is an Associate Professor and Program Coordinator of Electrical Engineering and Renewable Energy at Federation University Australia. His research interests include power electronics, renewable energy, and smart microgrids. Dr. Hu is an Associate Editor of IET Renewable Power Generation, an Editor of IEEE Transactions on Energy Conversion, and a Guest Editor of IEEE Transactions on Industrial Electronics for a Special Issue "Applications of Predictive Control in Microgrids".

Ka Wing Chan received the B.Sc. (Hons) and Ph.D. degrees in electronic and electrical engineering from the University of Bath, U.K., in 1988 and 1992, respectively. He currently is an Associate Professor and Associate Head in the Department of Electrical Engineering of the Hong Kong Polytechnic University. His research interests include power system stability, power grid integration, security, resilience and optimization, demand response management.

Syed Islam (Fellow, IEEE) received the B.Sc. degree in electrical engineering from the Bangladesh University of Engineering and Technology, Dhaka, Bangladesh, in 1979, and the M.Sc. and Ph.D. degrees in electrical power engineering from the King Fahd University of Petroleum and Minerals, Dhahran, Saudi Arabia, in 1983 and 1988, respectively.
He is currently the Dean of the School of Engineering, IT and Physical Sciences, Federation University Australia. He received the Dean's medallion for research at Curtin University, in 1999. He has been a Visiting Professor at the Shanghai University of Electrical Power Shanghai China. His current research interests include IoT, condition monitoring of transformers, wind energy conversion, and smart power systems.
Dr. Islam is a Fellow of IEEE, a Fellow of the Engineers Australia, a Fellow of IET. He received the IEEE Burke Haye's Faculty Recognition Award in 2000, the Sir John Madsen Medal in 2011 and 2014 for the Best Electrical Engineering Paper in Australia. He is a Founding Editor of the IEEE TRANSACTION ON SUSTAINABLE ENERGY and an Associate Editor of the IET Renewable Power Generation.